Wear 352-353 (2016) 1–8

Contents lists available at ScienceDirect

Wear

journal homepage: www.elsevier.com/locate/wear

Wear mapping and transitions in wheel and rail materials under different contact pressure and sliding velocity conditions

H.H. Ding, C.G. He, L. Ma, J. Guo, Q.Y. Liu, W.J. Wang*

Tribology Research Institute, State Key Laboratory of Traction Power, Southwest Jiaotong University, Chengdu 610031, China

ARTICLE INFO

Article history:
Received 10 December 2015
Received in revised form
16 January 2016
Accepted 20 January 2016
Available online 4 February 2016

Keywords:
Rolling–sliding
Rolling friction
Rail-wheel tribology
Fatigue
Mapping

ABSTRACT

The objective of this study is to construct wear mapping and transitions of wheel/rail materials under different contact pressure and sliding velocity conditions by means of comprehensive consideration of both wear rates and surface damage morphology of wheel/rail rollers. The results indicate that, both the wear rates of wheel rollers and the wear rates of rail rollers increase with contact pressure increasing. With sliding velocity increasing, the wheel wear rates show an increase trend and the rail wear rates decrease. Wear regime maps of wheel/rail materials are divided into two regions: mild wear regime and severe wear regime, and both the wear rates of wheel roller and the wear rates of rail roller are about 2.0×10^{-6} g/m on the transition boundaries. The wear mechanisms of the wheel and rail materials are significantly different and transform in different wear regimes. Based on the damage characteristics in different wear regimes, the wear mechanism maps of wheel and rail materials are constructed. Fatigue cracks of wheel material develop along with soft ferrite lines in the plastic deformation area. Furthermore, cracks on the rail rollers develop into the material a depth, then become parallel with the surface and turn towards it.

1. Introduction

Railway wheel/rail is a significant wearing part, which transfers the axle load force, traction force, braking force, etc. and guides the running direction of trains [1,2]. The increase of speed and axle load leads to more serious wear and fatigue damage on wheel and rail materials, accelerating the failure of them and posing a threat to the running security of railway [3–6]. Therefore, the wear and rolling contact fatigue (RCF) of wheel/rail should be studied and explored sufficiently under a wide range of speed and axle load conditions.

The wear and damage characteristics of wheel/rail materials have been extensively studied using various experimental and numerical methods [7–11]. Plenty of evidence is provided to show that the presence of a relatively low viscosity fluid is conducive to the initiation and growth of RCF cracks [12,13]. Adhesive and delamination wear mechanisms were thoroughly studied as well for the last decades. The results show that the material damage of adhesive wear is milder than that of delamination wear [5]. Furthermore, it is well known that insufficient adhesion will lead to wheels spinning and sliding on the rail surfaces when accelerating and braking, respectively, which causes severe surface damages of wheel and rail materials [14–19]. As reviewed in previous work, it is found that the wear and fatigue damage mechanisms of wheel and rail materials are complex and variable under different conditions. It is worth noting that wear maps are an easy method to discuss different wear and damage mechanisms and the transitions under a range of conditions [20–22].

It is well known that wear maps can be used to depict dominant wear processes and their severity of specific friction pairs [20]. There are two kinds of wheel and rail contacts in the field, namely rail head/wheel tread contact and rail gauge/wheel flange contact [23]. The former contact generally results in relatively low sliding velocity and mild damages of wheel and rail materials except for the spinning and sliding phenomena under poor adhesion conditions, while the latter contact leads to relatively high sliding velocity and serious damages. In previous research, wear maps were drawn purely according to wear rates, and they were divided into three regimes: mild, severe and catastrophic [24–30]. However, both the mild and the severe wear regimes were observed under the rail head/wheel tread contact condition. The difference of wear rates between the mild and the severe regimes is not as obvious as the difference between the severe and the catastrophic regimes [24]. Thus, in order to get a precise wear map under the rail head/wheel tread contact condition and identify the transition boundary between the mild and the severe wear regimes, not only the macro dates of wear rate but also the microanalyses like wear scars should be taken into consideration.

* Corresponding author. Tel.: +86 28 87634304.
E-mail address: wwj527@swjtu.cn (W.J. Wang).

http://dx.doi.org/10.1016/j.wear.2016.01.017
0043-1648/

Furthermore, as a coupled system, wheel and rail were discussed separately when constructing wear maps previously.

In this study, wear maps of wheel and rail materials under the rail head/wheel tread contact condition are drawn according to comprehensive analysis of both wear datas and damage morphologies from a series of wear tests under different contact pressure and sliding velocity conditions. Wear damage mechanisms and transitions were discussed, and the initiation and development of cracks on wheel and rail materials were illustrated as well.

2. Experimental details

Wear tests were carried out under the dry condition using a rolling–sliding wear testing apparatus which was composed of two rollers served as a wheel roller (upper specimen) and a rail roller (lower specimen). The wheel/rail rollers were powered and controlled by a DC motor. The geometric sizes of rollers were designed by means of Hertzian simulation rule [17]. The scheme of geometric size and the sampling positions of wheel/rail rollers are shown in Fig. 1.

The wheel and rail rollers were cut from the high speed wheel tread in China and rail head (U71Mn). Their chemical compositions in weight percentage are given in Table 1. The microstructures of wheel and rail materials are shown in Fig. 2. It is clear that the wheel material has a ferrite-pearlite microstructure which is composed of the mixture of ferrite and pearlite. The rail material has a pearlite microstructure (lamellae of cementite and ferrite).

According to Hertz stress formula [17], normal forces of 90, 120, 150, 180, and 220 N were adopted to produce average contact pressures of about 800, 880, 950, 1000, and 1070 MPa between wheel/rail rollers. Under each contact pressure condition, the rotational speeds of rail roller were 100, 300, 500 and 800 r/min, respectively. The slippage ratio of wheel/rail rollers was 2.38%. Therefore, the relative sliding velocities between wheel and rail rollers were 0.005, 0.015, 0.025, and 0.04 m/s, respectively. The number of cycles of rail roller was 2×10^5.

All experiments were carried out in the ambient condition (temperature: 18–23 °C, humidity: 50–70%). The rollers were ultrasonically cleaned in ethanol, dried, and weighed using an electronic balance (JA4103, 0.001 g) before and after testing. The wear rate of wheel/rail rollers is measured by mass loss (g) per rolling distance (m) of wheel or rail roller. The hardness of rollers was measured per 5×10^4 cycles (before, during, and after the test) using a Vickers hardness instrument (MVK-H21, Japan). The wear scar was inspected using a scanning electron microscope (SEM) (JSM-7001F, Japan). Sections were cut in the direction longitudinal to the rolling direction. Each section was mounted in resin, ground to 2000 grit, polished to 0.5 μm diamond, and etched with 4% nital, observed using SEM.

3. Results

3.1. Wear rates and surface hardness

Figs. 3 and 4 show the effects of contact pressure and sliding velocity on wear rates of wheel and rail materials. It is found from Fig. 3 that both the wear rate of wheel roller and the wear rate of rail roller increase markedly with an increase in contact pressure. When increasing the sliding velocity, the wear rate of wheel material shows an increasing trend (Fig. 4a). While, the wear rate of rail material exhibits a decline trend (Fig. 4b). Furthermore, more sensitive effects of changing sliding velocity on the wheel/rail wear rates are indicated under relatively higher contact pressure conditions. Namely, with the sliding velocity increasing, the increasing trend of wheel wear rate and the decreasing trend of rail wear rate become more intense under higher contact pressure conditions. Furthermore, both the wear rates of wheel material and the wear rates of rail material show no obvious change under the smallest pressure (800 MPa) condition (Fig. 4).

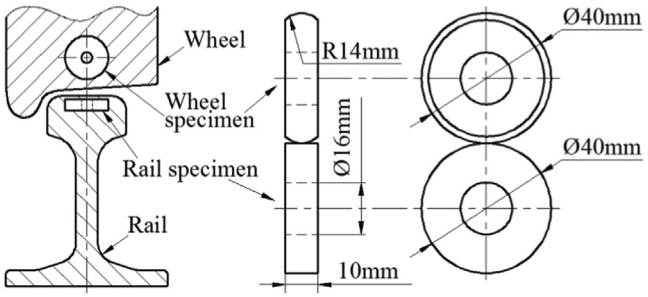

Fig. 1. Sampling positions and scheme of wheel and rail rollers.

Table 1
Chemical compositions of wheel and rail materials (wt%).

Roller	C	Si	Mn	P	S
Wheel	0.56–0.60	≤ 0.40	≤ 0.80	≤ 0.020	≤ 0.015
Rail	0.65–0.75	0.10–0.50	0.80–1.30	≤ 0.025	0.008–0.025

The surface hardness of wheel and rail rollers was measured 5 times (per 5×10^4 cycles) during one test. The hardness value during the test (i.e. the hardness of the plastically deformed material) is about 600 ± 50 $HV_{0.5}$ (wheel material) and 580 ± 50 $HV_{0.5}$ (rail material). The wheel/rail hardness ratio is obtained using dividing wheel hardness by rail hardness. The average value of wheel/rail hardness ratio over the testing time (Fig. 5) is gotten by averaging five wheel/rail hardness ratios of one test. It is clear that with the sliding velocity increasing, the average value of wheel/rail hardness ratio shows a decreasing tendency on the whole, which means that comparing with the rail material during and after the test (i.e. the plastically deformed rail material). The wheel material becomes relatively softer when increasing the sliding velocity. Therefore, the wear rate of wheel roller shows an upward trend (Fig. 4a) while the wear rate of rail roller decreases (Fig. 4b). Besides, it is noted that under the smallest pressure condition (Fig. 5), the decreasing tendency of the average value of wheel/rail hardness ratio is not evident. As a result, both the wear rate of wheel material and the wear rate of rail material show no obvious change when increasing the sliding velocity, shown in Fig. 4.

3.2. Surface damage behaviors

In order to further understand the effects of contact pressure and sliding velocity on the surface damage of wheel and rail materials, microscopic analysis is of greatest importance. Representative SEM micrographs of worn surfaces of wheel/rail rollers are shown in Figs. 6 and 7. It is evident that the surface damage morphology of wheel and rail materials is influenced by the contact pressure and the sliding velocity. Meanwhile, the influence of contact pressure is more obvious. Under lower contact pressure conditions, the surface damage of wheel (Fig. 6c–d) and rail (Fig. 7c–d) rollers is mild, while under higher pressure conditions, the surface damage is severe (Figs. 6a–b and 7a–b). Furthermore, the surface damage morphology of wheel rollers differs from that of rail rollers.